

# A New Improved Failure Criterion for Salt Rock Based on Energy Method

T. S. Hao<sup>1,2</sup> · W. G. Liang<sup>1,2</sup>

Received: 1 March 2015 / Accepted: 12 September 2015 / Published online: 21 September 2015  
© Springer-Verlag Wien 2015

**Abstract** A non-linear triple shear energy yield criterion for salt rock is presented in this paper. It is the development of the triple shear energy yield criterion, of which the Mohr–Coulomb criterion can be seen as a special case. The main factors affecting the primary strength of salt rock, such as the mean stress and the Lode angle, are considered in the non-linear triple shear energy yield criterion. The non-linear new criterion provides the non-linear change trend of salt strength both in the  $I_1$ – $J_2$  stress space and in the deviatoric plane. Comparative study between the non-linear criterion predictions and experimental results of salt rock shows that the non-linear triple shear energy yield criterion fits quite well with both conventional triaxial test data and the true triaxial test data. For Maha Sarakham salt, the predictive capability of the non-linear triple shear energy yield criterion is clearly better than that of some other criteria used by Sriapai, such as modified Lade criterion, 3-D Hoek, and Brown criterion, Drucker–Prager criterion et al. The availability of the non-linear triple shear energy yield criterion can also be confirmed by comparative analysis between theoretical values and experimental values for non-salt rocks. So the non-linear triple shear energy yield criterion is a general failure criterion for rocks fractured by shear stress.

**Keywords** Salt rock · Rock strength · Shear strain energy · Non-linear · Triple shear energy yield criterion

## List of symbols

|   |  |
|---|--|
| $c$                                     | Cohesion in Mohr–Coulomb criterion   |
| $c_1$                                   | Cohesion in $\sigma_1$ – $\sigma_3$ plane  |
| $D_1, D_2, D_3, D_4, D_5$               | Material constants   |
| $G$                                     | Shearing modulus of elasticity   |
| $I_1$                                   | First invariant of the stress  |
| $J_2$                                   | Second invariant of deviatoric stress  |
| $k$                                     | Limit of the maximal value of shear strain energy on failure plane   |
| $K$                                     | Sum of the limit of the maximal value of shear strain energy for an element  |
| $N$                                     | Power parameter  |
| $w_1, w_2, w_3$                         | Maximal value of shear strain energy on the $\tau_1$ plane, on the $\tau_2$ plane, on the $\tau_3$ plane, respectively |
| $\alpha_1, \alpha_2, \alpha_3$          | Angle of the $\tau_1$ plane, the $\tau_2$ plane, the $\tau_3$ plane, respectively                                      |
| $\beta$                                 | Dimensional constant with the same units as $I_1$  |
| $\sigma_1, \sigma_2, \sigma_3$          | Major, intermediate and minor principal stress, respectively   |
| $\sigma_{n1}, \sigma_{n2}, \sigma_{n3}$ | Normal stress acting on the $\tau_1$ plane, on the $\tau_2$ plane, on the $\tau_3$ plane, respectively                 |
| $\sigma_m$                              | Mean stress  |
| $\tau_1$                                | Maximum principal shear stress   |
| $\tau_2$                                | Intermediate or minimum principal shear stress   |
| $\tau_3$                                | Intermediate or minimum principal shear stress   |
| $\theta$                                | Lode angle   |

✉ W. G. Liang  
master\_lwg@hotmail.com

<sup>1</sup> College of Mining Engineering, Taiyuan University of Technology, Taiyuan, Shanxi, China

<sup>2</sup> Key Lab of In-situ Property-Improving Mining of Ministry of Education, Taiyuan, Shanxi, China

|                                   |   |
|-----------------------------------|---|
| $\varphi_1, \varphi_2, \varphi_3$ | Maximal friction angle in $\sigma_1$ – $\sigma_3$ plane, in $\sigma_1$ – $\sigma_2$ plane, in $\sigma_2$ – $\sigma_3$ plane, respectively |
| $\varphi$                         | Friction angle in Mohr–Coulomb criterion  |

## 1 Introduction

Rock salt deposit is considered as an ideal medium for natural gas and oil storage because of its low permeability, self-healing of damage, and strong creep characteristics. With the demand of “west to east pipeline” project in China, the construction of natural gas storage in salt formations has been started for several years. In order to increase gas storage capabilities and provide operators with improved geotechnical design and operating guidelines for these caverns, tightness analyses, and stability evaluation of these salt caverns are basically demanded. A main factor that often jeopardizes the cavern tightness and stability is the potential for salt dilation. During the practical operation of storage caverns running, shear stress can be induced in the salt around the caverns by the difference between the storage pressure acting on the cavern walls and the in situ stress in the surrounding salt. Once the shear stresses exceed the strength of the salt due to too aggressive extraction of gas from the cavern, micro-fractures could be generated in the salt. Progressive micro-fracturing may result in the growth of salt volume, which is referred to as salt dilation. The salt dilation not only increases the porosity of salt, reduces the strength of salt, but also accelerates cavern closure or even cause the roof and wall to collapse. Therefore, the salt dilation is a crucial factor for the design and development of storage caverns, and scientific and reasonable determination of salt strength is needed for predicting the onset of salt dilation.

Many scholars studied the problems in relative fields, e.g., constant strain rate tests (Spiers et al. 1988; Hatzor and Heyman 1997) were performed on salt specimens taken from different areas to develop salt dilatancy criterion. Ratigan and Vogt (1991) developed a criterion from evaluation of volumetric strain rates for WIPP and Avery Island, Louisiana, domal salt creep tests were performed at room temperature. Hunsche and Albrecht (1990) and Hunsche (1993) used the results of 14 true triaxial tests on cubic specimens of salt from the Asse Salt Mine to develop a compressibility/dilatancy boundary, and pointed out that the failure strength of salt is about 30 % less for tests subjected to triaxial extension stress states compared with triaxial compression stress states. DeVries et al. (2002, 2005) developed a continuum damage criterion to determine the minimum operation pressure for compressed natural gas storage caverns in bedded salt formations,

thereby guaranteeing the roof stability of salt caverns. Liang et al. (2011) investigated the effect of strain rate on the mechanical properties of salt rock, and pointed out that the strength of salt rock is only slightly affected by loading strain rate. The elastic modulus slightly increases with strain rate, but the increment is small. The influence of cyclic loading on mechanical properties of salt rock under uniaxial and triaxial compressive conditions was also studied (Fuenkajorn and Phueakphum 2010; Ma et al. 2013). The results showed that the cyclic loading can decrease the salt strength by up to 30 %, depending on the maximum applied load and the number of loading cycles. In general, it was found that the mean stress and the stress geometry, as described by the Lode angle, are the main factors affecting the primary strength of salt rock.

As described above, the accurate determination of salt strength is still a difficult problem, and a unified method for predicting the onset of the salt dilation was not formed. Most of criteria in the past were developed by fitting testing results to the existing strength criteria, such as the popular Mohr–Coulomb, the Hoek–Brown criterion, and Drucker–Prager criteria et al. But the Mohr–Coulomb criterion and the Hoek–Brown criterion, which does not consider intermediate principal stress at failure, cannot describe the salt strength beyond the triaxial compression condition. Likewise, the Drucker–Prager criterion, as an extended version of the von Mises criterion, is not able to describe the salt strength accurately (Liu et al. 2011; Sriapai et al. 2013). There are around 20 rock failure criteria available (Yu et al. 2002) for predicting the strength of rocks and each one is particularly suitable for one rock type or some rock types. Which failure criterion is the best to be used for fitting the previous testing results and describing the mechanical behavior of the salt rock?

The main motivation of the paper is to present a new accurate criterion with clear mechanism to describe the mechanical properties of salt rock and determine dilatancy boundary of salt rock. A basic concept obtained from the general law of thermodynamics is that the intrinsic feature for salt deformation is the transformation of energy, which can reflect the change of mechanical properties for salt rock. However, rare effort has been made to investigate the strength of salt rock by strain energy. So, the shear energy yield theory (Gao et al. 2007; Zheng and Kong 2010) is introduced into the development of the new criterion. Comparative study between the new criterion predictions and experimental results is also performed in this paper.

## 2 Calculations of Shear Strain Energy

The failure of salt rock is mainly caused by the shear stress (Liang et al. 2007) and the shear strain plays a key role in the salt failure, on the other hand, the volumetric strain has

little effect on the salt failure. Therefore, the influence of the volumetric strain to the salt failure is overlooked during development of failure criteria.

An element of salt rock for analysis is illustrated in Fig. 1a, in which  $\sigma_1$ ,  $\sigma_2$ , and  $\sigma_3$  is major, intermediate and minor principal stresses, respectively. One method, we used for calculating the shear strain energy is to use the principal shear stresses  $\tau_1$ ,  $\tau_2$ ,  $\tau_3$ , and the normal stress  $\sigma_{n1}$ ,  $\sigma_{n2}$ ,  $\sigma_{n3}$  acting on the same planes, respectively (Yu et al. 2002), shown in Fig. 1b–d.

As illustrated in Fig. 1b, for element of rock materials including salt rock, failure usually happens on the plane oriented at  $\alpha_1$  ( $\alpha_1 = 45^\circ + \varphi_1/2$ ) to the direction of principal stress. The normal stress and shear stress acting on the failure plane can be solved by Mohr’s circle, and are written as

$$\begin{aligned} \sigma_{n1} &= \frac{\sigma_1 + \sigma_3}{2} + \frac{\sigma_1 - \sigma_3}{2} \sin \varphi_1 \\ \tau_1 &= \frac{\sigma_1 - \sigma_3}{2} \cos \varphi_1 \end{aligned} \quad (1)$$

where  $\sigma_{n1}$  is the effective normal stress acting on the failure plane,  $\tau_1$  is the principal shear stress acting on the failure plane and  $\varphi_1$  is the maximal friction angle in  $x$ - $z$  plane.

Thus, the maximal value of shear strain energy on the failure plane is obtained, involving the effects of frictions on the failure plane, and can be written as

$$\begin{aligned} w_1 &= \frac{(\tau_1 + \sigma_{n1} \tan \varphi_1)^2}{2G} \\ &= \frac{1}{2G} \left( \frac{\sigma_1 - \sigma_3}{2 \cos \varphi_1} + \frac{\sigma_1 + \sigma_3}{2} \tan \varphi_1 \right)^2 \end{aligned} \quad (2)$$

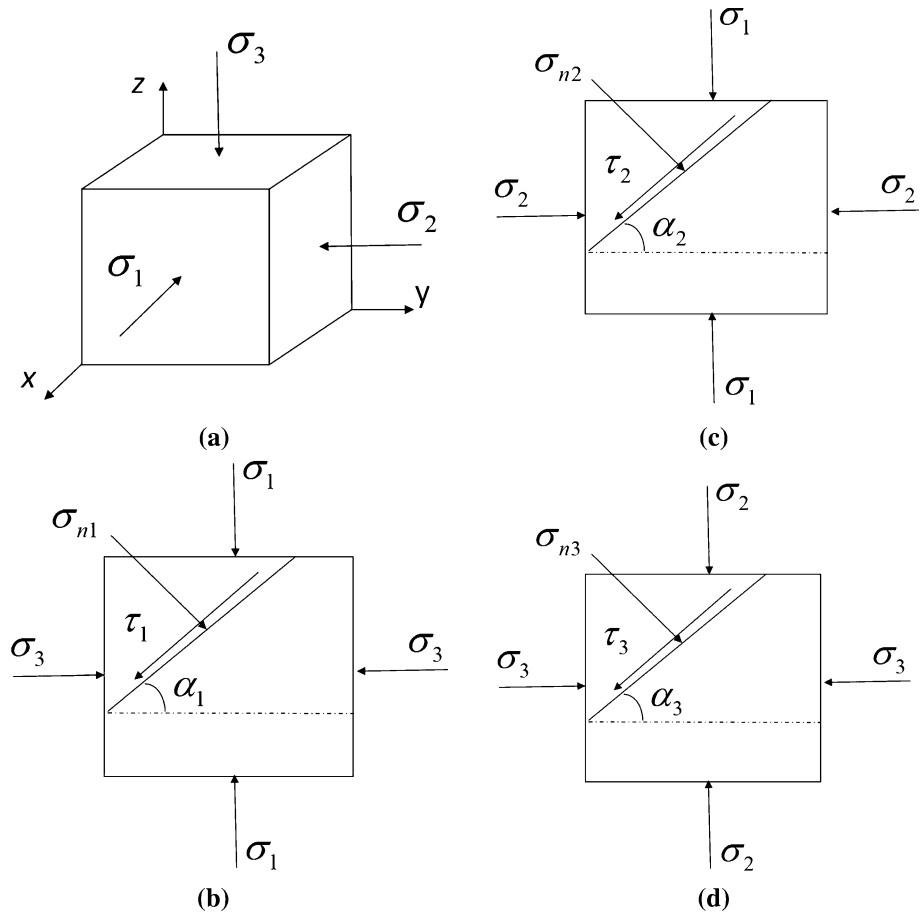
where  $G$  is the shearing modulus of elasticity.

In the opinion of the triple shear energy yield theory, the shear strain energy is also induced in  $x$ - $y$  plane and in  $y$ - $z$  plane. In a similar manner, the maximal values of shear strain energy in  $x$ - $y$  plane and in  $y$ - $z$  plane are derived as

$$\begin{aligned} w_2 &= \frac{(\tau_2 + \sigma_{n2} \tan \varphi_2)^2}{2G} \\ &= \frac{1}{2G} \left( \frac{\sigma_1 - \sigma_2}{2 \cos \varphi_2} + \frac{\sigma_1 + \sigma_2}{2} \tan \varphi_2 \right)^2 \end{aligned} \quad (3)$$

$$\begin{aligned} w_3 &= \frac{(\tau_3 + \sigma_{n3} \tan \varphi_3)^2}{2G} \\ &= \frac{1}{2G} \left( \frac{\sigma_2 - \sigma_3}{2 \cos \varphi_3} + \frac{\sigma_2 + \sigma_3}{2} \tan \varphi_3 \right)^2 \end{aligned} \quad (4)$$

**Fig. 1** Schematic diagram of the principal shear stresses. **a** The salt element for analysis, **b** the principal shear stresses  $\tau_1$  in  $x$ - $z$  plane, **c** the principal shear stresses  $\tau_2$  in  $x$ - $y$  plane, **d** the principal shear stresses  $\tau_3$  in  $y$ - $z$  plane



Further,  $w_1, w_2, w_3$  can also be written in terms of stress invariants as

$$\begin{aligned}
 w_1 &= \frac{1}{2G \cos^2 \varphi_1} \left( \frac{I_1}{3} \sin \varphi_1 + \sqrt{J_2} \cos \theta - \frac{\sqrt{3J_2}}{3} \sin \theta \sin \varphi_1 \right)^2 \\
 w_2 &= \frac{1}{2G \cos^2 \varphi_2} \left( \frac{I_1}{3} \sin \varphi_2 + \sqrt{J_2} \cos \left( \theta + \frac{\pi}{3} \right) + \frac{\sqrt{3J_2}}{3} \sin \left( \theta + \frac{\pi}{3} \right) \sin \varphi_2 \right)^2, \\
 w_3 &= \frac{1}{2G \cos^2 \varphi_3} \left( \frac{I_1}{3} \sin \varphi_3 + \sqrt{J_2} \cos \left( \theta - \frac{\pi}{3} \right) + \frac{\sqrt{3J_2}}{3} \sin \left( \theta - \frac{\pi}{3} \right) \sin \varphi_3 \right)^2
 \end{aligned} \tag{5}$$

where  $J_2$  is the second invariant of the deviatoric stress,  $I_1$  is the first invariant of the stress and  $\theta$  is the Lode angle.

### 3 Triple Shear Energy Yield Criterion

#### 3.1 Single Shear Energy Yield Criterion

The single shear energy yield criterion points out that the shear damage on failure plane is only caused by the maximal values of shear strain energy on the same plane. When the maximal value of shear strain energy reaches a certain value, shear fracture occurs on the failure plane. Thus, the single shear energy yield criterion can be expressed as

$$\begin{aligned}
 w_1 &= \frac{(\tau_1 + \sigma_{n1} \tan \varphi_1)^2}{2G} \\
 &= \frac{1}{2G} \left( \frac{\sigma_1 - \sigma_3}{2 \cos \varphi_1} + \frac{\sigma_1 + \sigma_3}{2} \tan \varphi_1 \right)^2 = k,
 \end{aligned} \tag{6}$$

where  $k$  is the limit of the maximal value of shear strain energy in  $x$ - $z$  plane.

If we assume that  $\tau_1$  is equal to the cohesion of salt when  $\sigma_{n1} = 0$  (Coulomb 1776). That is

$$\tau_1 = c_1, \quad \text{when } \sigma_{n1} = 0, \tag{7}$$

where  $c_1$  is the cohesion of salt in  $x$ - $z$  plane.

Then, the value of  $k$  can be derived by substituting Eq. (7) into Eq. (6), and is written as

$$k = \frac{c_1^2}{2G}. \tag{8}$$

We observe that  $\varphi_1 = \varphi$  ( $\varphi$  is the internal friction angle of salt defined by the Mohr–Coulomb criterion) and  $c_1 = c$  ( $c$  is the cohesion of salt defined by the Mohr–Coulomb criterion). By substituting these values into the first formula of Eq. (5), the expression is rewritten in terms of stress invariants as

$$\sqrt{J_2} \left( \cos \theta - \frac{1}{\sqrt{3}} \sin \theta \sin \varphi \right) + \frac{I_1}{3} \sin \varphi = c \cos \varphi \tag{9}$$

Equation (9) is obviously just the famous Mohr–Coulomb criterion. The Mohr–Coulomb criterion is not only a single shear stress criterion but also the single shear energy yield criterion.

#### 3.2 Triple Shear Energy Yield Criterion

Although the Mohr–Coulomb criterion has been widely applied for many rocks, it is evident that the Mohr–Coulomb criterion incorporates the only shear strain energy on the failure plane ( $x$ - $z$  plane) and does not consider intermediate principal stress at failure as described previously. Sriapai et al. (2013) has confirmed that the intermediate principal stress does have great effect on the shear fracture of salt. For more accurate prediction of the mechanical properties of salt rock, we take into account the shear strain energy on three planes ( $x$ - $z$  plane,  $x$ - $y$  plane,  $y$ - $z$  plane) and assume that each of the maximal value of shear strain energy reaches its limit when the shear fracture occurs on the failure plane. That is, the sum of  $w_1, w_2, w_3$  reaches its limit. Thus, the triple shear energy yield criterion can be given as

$$w_1 + w_2 + w_3 = K, \tag{10}$$

where  $K$  is the sum of the limit of  $w_1, w_2, w_3$ .

Substituting Eq. (5) into Eq. (10), the expression of Eq. (10) is rewritten as

$$\begin{aligned}
 &\frac{1}{2G \cos^2 \varphi_1} \left( \frac{I_1}{3} \sin \varphi_1 + \sqrt{J_2} \cos \theta - \frac{\sqrt{3J_2}}{3} \sin \theta \sin \varphi_1 \right)^2 \\
 &+ \frac{1}{2G \cos^2 \varphi_2} \left( \frac{I_1}{3} \sin \varphi_2 + \sqrt{J_2} \cos \left( \theta + \frac{\pi}{3} \right) + \frac{\sqrt{3J_2}}{3} \sin \left( \theta + \frac{\pi}{3} \right) \sin \varphi_2 \right)^2 \\
 &+ \frac{1}{2G \cos^2 \varphi_3} \left( \frac{I_1}{3} \sin \varphi_3 + \sqrt{J_2} \cos \left( \theta - \frac{\pi}{3} \right) + \frac{\sqrt{3J_2}}{3} \sin \left( \theta - \frac{\pi}{3} \right) \sin \varphi_3 \right)^2 = K
 \end{aligned} \tag{11}$$

The value of  $K$  depends on the mechanical properties of salt and can be determined by performing conventional triaxial compression testing of salt under the conditions:

$$\theta = 30^\circ, \quad \sigma_1 > \sigma_2 = \sigma_3; \quad \varphi_3 = 0, \quad \varphi_1 = \varphi_2 = \varphi \tag{12}$$

and  $K$  is given in a similar way of Eq. (8):

$$K = \frac{c^2}{G}, \tag{13}$$

where  $c$  is the cohesion of salt,  $c = c_1$ .

The relations among  $\varphi_1, \varphi_2, \varphi_3$  can be easily obtained by Mohr’s circles which is plotted in Fig. 2 and are given as follows:

$$\begin{aligned}
 \sin \varphi_2 &= \frac{(1 - \sqrt{3} \tan \theta) \sin \varphi}{2 - \sin \varphi - \sqrt{3} \tan \theta \sin \varphi}, \\
 \sin \varphi_3 &= \frac{(1 + \sqrt{3} \tan \theta) \sin \varphi}{2 - \sin \varphi - \sqrt{3} \tan \theta \sin \varphi}
 \end{aligned} \tag{14}$$

where  $\varphi = \varphi_1$ .

Finally, by substituting Eqs. (13) and (14) into Eq. (11) and rearranging, the triple shear energy yield criterion can be given in a simplified expression:

$$\sqrt{J_2} \left( \cos \theta - \frac{1}{\sqrt{3}} \sin \theta \sin \varphi \right) + \frac{I_1}{3} \sin \varphi = 2c \cos \varphi \sqrt{\frac{1 - \sqrt{3} \tan \theta \sin \varphi}{3 + 3 \tan^2 \theta - 4\sqrt{3} \tan \theta \sin \varphi}} \quad (15)$$

It is worth noting that the triple shear energy yield criterion (Eq. (15)) has a similar expression to the Mohr–Coulomb criterion (Eq. (9)). Both of the two criteria has a linear relation in  $I_1$ – $J_2$  stress space; the left-hand side of the two criteria is the same, but the right-hand side of the triple shear energy yield criterion has an additional term, which is a function of  $\theta$  (Lode angle); when  $\theta = 30^\circ$  or  $\theta = -30^\circ$ , the triple shear energy yield criterion reduces to the Mohr–Coulomb criterion, but that is not the same case when  $\theta \neq 30^\circ$  (or  $-30^\circ$ ), the right-hand side of the triple

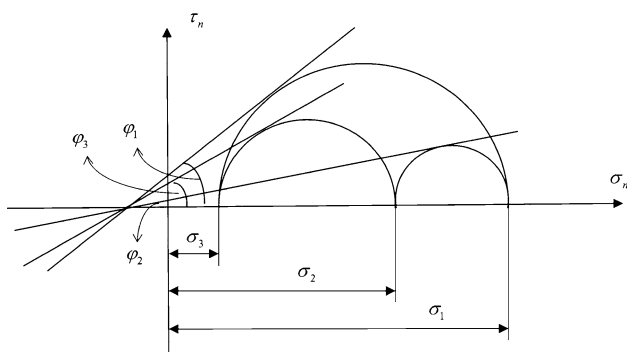


Fig. 2 The relations among  $\varphi_1, \varphi_2, \varphi_3$  in the Mohr's circles

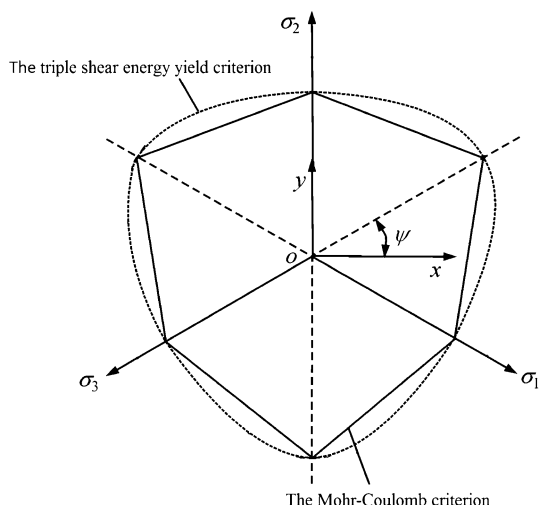


Fig. 3 Illustration of the triple shear energy yield criterion and the Mohr–Coulomb criterion plotted in the deviatoric plane

shear energy yield criterion is greater than that of the Mohr–Coulomb criterion. Limit loci of the two criteria in the deviatoric plane are plotted vividly in Fig. 3. The limit locus of the triple shear energy yield criterion is curved and the significant effect of intermediate principal stress becomes clear with parameter  $\theta$  (Lode angle) changing from  $-30^\circ$  to  $30^\circ$ . This is confirmed by the true triaxial compression test data produced by Hunsche and Albrecht (1990).

### 4 Non-Linear Triple Shear Energy Yield Criterion

The linear triple shear energy yield criterion is described above (Eq. (15)). But the confined compression tests and confined tension tests on bedded salt in the Appalachian Basin conducted by DeVries et al. (2005) indicated that salt strength varies nonlinearly in the  $I_1$ – $J_2$  stress space. Their parameters are shown in Table 1. So a new non-linear triple shear energy yield criterion can be proposed for salt rock as follows:

$$\sqrt{J_2} = \frac{D_1 \left( \frac{I_1}{\text{sgn}(I_1)\beta} \right)^N}{\sqrt{3} \cos \theta - D_5 \sin \theta} + \frac{D_2 \left( \frac{1 - D_3 \tan \theta}{3 + 3 \tan^2 \theta - D_4 \tan \theta} \right)^{\frac{1}{2}}}{\sqrt{3} \cos \theta - D_5 \sin \theta} \quad (16)$$

where  $N$  is a power less than or equal to 1 and  $\beta$  is a dimensional constant with the same units as  $I_1$ ;  $D_1$ – $D_5$  are the constants of materials.

The curves computed by the non-linear triple shear energy yield criterion and test data points of bedded salt in the Appalachian Basin are compared in Fig. 4. From the test data,  $\beta = 0.515, N = 0.86, D_1 = 0.303, D_2 = 3.9, D_3 = 0.908, D_4 = 3.63, D_5 = 0.524$ . It is obviously that

Table 1 The results of the triaxial compressive tests for Cayuta salt conducted by DeVries et al. (2005)

| Specimen ID                                    | $\sigma_m$ (MPa) | $\sigma_1 - \sigma_3$ (MPa) | Dilation stress state |                    |                     |
|--|------------------|-----------------------------|-----------------------|--------------------|---------------------|
|  |                  |                             | $I_1$ (MPa)           | $\sqrt{J_2}$ (MPa) | $\psi$ ( $^\circ$ ) |
| Triaxial extension tests on virgin specimens   |                  |                             |                       |                    |                     |
| BAL1/151/4                                     | 5.2              | 7.5                         | 15.6                  | 4.33               | -30                 |
| BAL1/152/5                                     | 7.1              | 8                           | 21.3                  | 4.62               | -30                 |
| BAL1/124/4                                     | 10.6             | 9.5                         | 31.8                  | 5.48               | -30                 |
| BAL1/152/3                                     | 14.2             | 12.5                        | 42.6                  | 7.22               | -30                 |
| BAL1/124/1                                     | 17.7             | 14.5                        | 53.1                  | 8.37               | -30                 |
| BAL1/152/1                                     | 21.2             | 15.5                        | 63.6                  | 8.95               | -30                 |
| Triaxial compression tests on virgin specimens |                  |                             |                       |                    |                     |
| BAL1/151/5                                     | 6.80             | 12.00                       | 20.40                 | 6.93               | 30                  |
| BAL1/124/5                                     | 10.30            | 15.00                       | 30.90                 | 8.66               | 30                  |
| BAL1/124/3                                     | 17.20            | 20.00                       | 51.60                 | 11.55              | 30                  |
| BAL1/152/2                                     | 20.70            | 22.00                       | 62.10                 | 12.70              | 30                  |

the test result fits with the non-linear triple shear energy yield criterion very well. The new non-linear criterion provides a significant improvement over the linear criterion in its ability to represent the test data.

## 5 Experimental Comparisons

### 5.1 Comparative Study for Maha Sarakham Salt

The failure surface of the non-linear triple shear energy yield criterion is determined above. This can be confirmed by the true triaxial compression test data on Maha Sarakham salt formation in the Khorat basin, northeast Thailand produced by Sriapai et al. (2013). Their results are listed in Table 2. The Sriapai et al. reported that the effect of  $\sigma_2$  on the failure stress  $\sigma_1$  for all levels of  $\sigma_3$  is non-linear. The modified Lade and 3-D Hoek and Brown criteria overestimate the strength at all levels of  $\sigma_3$ . The Coulomb and Hoek and Brown criteria cannot describe the salt strengths beyond the condition where  $\sigma_2 = \sigma_3$ , as they cannot incorporate the effects of  $\sigma_2$ . Both circumscribed and inscribed Drucker–Prager criteria, which ignore the differences in salt strength at triaxial compression and triaxial extension stress conditions, severely underestimate  $\sigma_1$  at failure for all stress conditions, showing the largest mean misfit of 19.5 MPa. The best criterion used by Sriapai is the modified Wiebols and Cook criterion, of which the mean misfit is of 3.8 MPa. The details can be seen in the paper (Sriapai et al. 2013).

Figure 5 compares the non-linear triple shear energy yield criterion predictions with the test results on Maha Sarakham salt for  $\sigma_3 = 0, 1, 3, 5$  and 7 MPa. The fitting parameters of Maha Sarakham salt are  $\beta = 0.515$ ,  $N = 0.86$ ,  $D_1 = 0.442$ ,  $D_2 = 11.133$ ,  $D_3 = 0.56$ ,

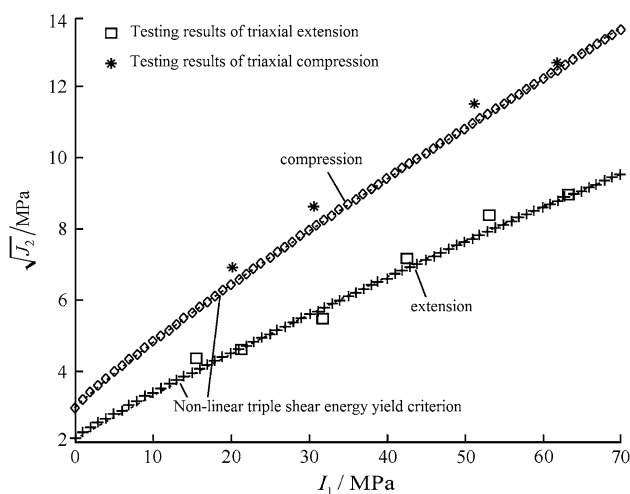


**Fig. 4** Illustration of the fitting results by the non-linear triaxial shear energy yield criterion with the triaxial testing data of Cayuta salt produced by DeVries

$D_4 = 2.24$ ,  $D_5 = 0.766$ . Analysis of the above Comparisons shows that the non-linear triple shear energy yield criterion fits well with most of experimental data, particularly under high  $\sigma_3$  values. As listed in Table 2, the error of  $\sqrt{J_2}$  between theoretical values by the non-linear triple shear energy yield criterion and experimental values for most test data is small. The largest error of  $\sqrt{J_2}$  occurs at  $\sigma_3 = 0$  MPa is of 4.7 MPa, and the mean misfit at  $\sigma_3 = 0$  is only 3.8 MPa, which is much less than that of other criteria produced by Sriapai. The smallest error of  $\sqrt{J_2}$  occurs at  $\sigma_3 = 5$  MPa and is only of 0.25 MPa. The non-linear triple shear energy yield criterion does show obviously a more accurate prediction of salt strength than that of other criteria used by Sriapai.

### 5.2 Comparative Analysis for Non-Salt Rocks

Although the main objective of this study is to provide a new improved failure criterion for salt rock, a lot of experiments (Handin et al. 1967; Mogi 1979; Michelis 1985; Gao and Tao 1993; Oku et al. 2007; HHaimson and Chang 2000; Lee and Haimson 2011) have been performed on many non-salt rocks, in which the damage of these rocks can also be seen as the results of shear fracture. It is needed to verify the availability of the non-linear triple shear energy yield criterion for non-salt rocks. In this study, we picked up three types of rocks: Dunham dolomite, Mizuho trachyte, Naxos marble.

The true triaxial testing results of Dunham dolomite and Mizuho trachyte are given by Mogi (1979) and are shown in Tables 3 and 4. Fitting parameters of the two rocks are calculated for the non-linear triaxial shear energy yield criterion and listed in Table 6.

As seen in Fig. 6, the non-linear triaxial shear energy yield criterion fits very well to the test data for Dunham dolomite, under both higher and lower  $\sigma_3$  values. Although the errors of some points reach 20–30 MPa, the error between theoretical values and experimental values for most test data is small. The smallest error of  $\sqrt{J_2}$  occurs at  $\sigma_3 = 45$  MPa and is only of 0.34 MPa. The lines calculated by the non-linear triaxial shear energy yield criterion and test data points of Mizuho trachyte are compared in Fig. 7. The non-linear triaxial shear energy yield criterion also gives a good prediction for the strength of Mizuho trachyte. The smallest error of  $\sqrt{J_2}$  occurs at  $\sigma_3 = 45$  MPa and is only of 0.11 MPa.

The Experimental values of Naxos marble given by Michelis (1985) are listed in Table 5. Fitting parameters of Naxos marble are also shown in Table 6. Analysis of the test data of Naxos marble shows that the error between theoretical values and experimental values for most test data is also small.

**Table 2** The results of the true triaxial compressive tests for Maha Sarakham salt conducted by Sriapai et al. (2013)

| Specimen ID | Failure stresses |                  |                  | $\psi$<br>(°) | $\sigma_m$ (MPa) | $\sqrt{J_2}$ (MPa)<br>Experimental | $\sqrt{J_2}$ (MPa)<br>Theoretical | Errors (MPa) |
|-------------|------------------|------------------|------------------|---------------|------------------|------------------------------------|-----------------------------------|--------------|
|             | $\sigma_3$ (MPa) | $\sigma_2$ (MPa) | $\sigma_1$ (MPa) |               |                  |                                    |                                   |              |
| 56          | 0                | 0                | 23               | 30            | 7.67             | 13.28                              | 15.41                             | 2.13         |
| 7           | 0                | 10               | 36.2             | 14.49         | 15.4             | 15.67                              | 18.73                             | 3.06         |
| 55          | 0                | 25               | 43.1             | -5.28         | 22.7             | 14.61                              | 19.95                             | 5.34         |
| 42          | 0                | 35.1             | 35.1             | -30           | 23.4             | 14.33                              | 19.05                             | 4.72         |
| 20          | 1                | 1                | 26.5             | 30            | 28.5             | 14.72                              | 17.48                             | 2.76         |
| 22          | 1                | 7                | 43.2             | 22.45         | 51.2             | 21.04                              | 22.31                             | 1.27         |
| 23          | 1                | 14               | 56.1             | 16.96         | 71.1             | 24.88                              | 25.79                             | 0.91         |
| 54          | 1                | 25               | 60.4             | 6.32          | 86.4             | 22.67                              | 25.94                             | 3.27         |
| 61          | 3                | 3                | 45.1             | 30            | 51.1             | 24.31                              | 25.59                             | 1.28         |
| 53          | 3                | 7                | 55               | 26.04         | 65               | 27.76                              | 27.45                             | 0.31         |
| 52          | 3                | 10               | 61               | 23.65         | 74               | 29.58                              | 28.98                             | 0.6          |
| 5           | 3                | 14               | 66               | 20.59         | 83               | 30.36                              | 29.98                             | 0.38         |
| 27          | 5                | 5                | 58.6             | 30            | 68.6             | 30.95                              | 31.61                             | 0.66         |
| 28          | 5                | 14               | 71.2             | 22.8          | 90.2             | 33.23                              | 32.53                             | 0.7          |
| 29          | 5                | 21               | 79.2             | 18.18         | 105.2            | 34.23                              | 33.98                             | 0.25         |
| 47          | 5                | 30               | 87.4             | 12.79         | 122.4            | 34.68                              | 35.39                             | 0.71         |
| 1           | 7                | 7                | 66.3             | 30            | 80.3             | 34.24                              | 35.46                             | 1.22         |
| 13          | 7                | 14               | 78.1             | 24.88         | 99.1             | 37.12                              | 35.71                             | 1.41         |
| 19          | 7                | 24               | 92.4             | 19.16         | 123.4            | 40.09                              | 38.59                             | 1.5          |
| 25          | 7                | 40               | 106.4            | 10.98         | 153.4            | 40.63                              | 40.95                             | 0.32         |
| Average     |                  |                  |                  |               |                  |                                    |                                   | 1.64         |

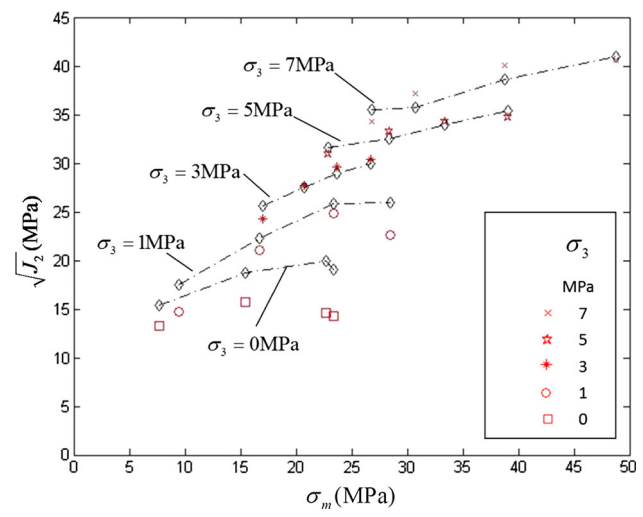


**Fig. 5** Comparisons between the true triaxial test data (points) of Maha Sarakham salt produced by Sriapai and the non-linear triaxial shear energy yield criterion prediction (lines) in terms of  $\sqrt{J_2}$

**6 Conclusions**

1. Many failure criteria for salt rock material have been developed in the past. But some of them usually overestimate or underestimate salt strength, such as the

Mohr–Coulomb criterion, the Drucker–Prager criterion; some of them obtained only by testing results lack good theoretical basis, such as the Lade criterion (Lade and Duncan 1975). The non-linear triple shear energy yield criterion proposed in this paper can be regard as a perfect application of energy method. It not only reflects the non-linear change trend of salt strength in the  $I_1$ – $J_2$  stress space, but also reveals the non-linear locus of salt strength in the deviatoric plane influenced by the intermediate principal stress. This can be confirmed by other researchers (Chang and Haimson 2012).

2. The non-linear triple shear energy yield criterion fits quite well with most of experimental data produced by Sriapai. It presents more accurate predictions of salt strength than that of some other criteria, such as the Mohr–Coulomb, the Hoek–Brown criterion and Drucker–Prager criteria et al. The error of salt strength between theoretical values by the non-linear triple shear energy yield criterion and experimental values is small.

3. The non-linear triple shear energy yield criterion incorporates the main factors influencing on the primary strength of salt rock, such as the mean stress and the Lode angle. It provides a significant improvement over the linear criterion in its ability to represent

**Table 3** The results of the true triaxial compressive tests for Dunham dolomite conducted by Mogi (1979)

| Failure stresses |                  |                  | $\psi$<br>(°) | $\sigma_m$ (MPa) | $\sqrt{J_2}$ (MPa)<br>Experimental | $\sqrt{J_2}$ (MPa)<br>Theoretical | Errors (MPa) |
|------------------|------------------|------------------|---------------|------------------|------------------------------------|-----------------------------------|--------------|
| $\sigma_3$ (MPa) | $\sigma_2$ (MPa) | $\sigma_1$ (MPa) |               |                  |                                    |                                   |              |
| 25               | 25               | 400              | 30.0          | 150              | 216.51                             | 236.74                            | 20.23        |
| 25               | 67.64            | 473.5            | 25.06         | 188.713          | 234.97                             | 241.92                            | 6.95         |
| 25               | 91.18            | 500              | 22.61         | 205.39           | 237.57                             | 240.65                            | 3.08         |
| 25               | 135              | 552.9            | 18.61         | 237.63           | 245.42                             | 241.97                            | 3.45         |
| 25               | 176.5            | 573.5            | 14.49         | 258.33           | 237.41                             | 236.33                            | 1.08         |
| 25               | 232.4            | 594.1            | 8.90          | 283.83           | 225.34                             | 229.83                            | 4.49         |
| 25               | 300              | 626.5            | 2.83          | 317.17           | 219.40                             | 228.21                            | 8.81         |
| 45               | 45               | 488.2            | 30.0          | 192.73           | 255.88                             | 275.74                            | 19.86        |
| 45               | 100              | 561.8            | 24.44         | 235.6            | 267.56                             | 272.64                            | 5.08         |
| 45               | 123.5            | 582.4            | 22.23         | 250.3            | 266.88                             | 269.04                            | 2.16         |
| 45               | 155.88           | 608.8            | 19.30         | 269.89           | 265.38                             | 265.04                            | 0.34         |
| 45               | 179.4            | 608.8            | 16.81         | 277.73           | 253.913                            | 257.24                            | 3.327        |
| 45               | 238.2            | 670.6            | 12.45         | 317.93           | 261.81                             | 259.60                            | 2.21         |
| 45               | 267              | 670.5            | 9.51          | 327.5            | 249.97                             | 253.08                            | 3.11         |
| 45               | 300              | 658.8            | 5.58          | 334.6            | 231.84                             | 243.50                            | 11.66        |
| 65               | 65               | 567.6            | 30.0          | 232.53           | 290.18                             | 309.32                            | 19.14        |
| 65               | 117.6            | 629.4            | 25.16         | 270.67           | 296.27                             | 301.78                            | 5.51         |
| 65               | 150              | 644.11           | 22.19         | 286.37           | 287.38                             | 291.79                            | 4.41         |
| 65               | 205.9            | 690              | 17.59         | 320.3            | 285.35                             | 284.77                            | 0.58         |
| 65               | 302.9            | 729.4            | 9.308         | 365.77           | 264.70                             | 270.11                            | 5.41         |
| 65               | 373.5            | 711.76           | 1.52          | 383.42           | 232.38                             | 252.93                            | 20.55        |
| 85               | 85               | 623.5            | 30.0          | 264.5            | 310.90                             | 334.82                            | 23.92        |
| 85               | 132              | 688.2            | 25.98         | 301.73           | 321.69                             | 328.99                            | 7.3          |
| 85               | 223              | 752.9            | 18.72         | 353.63           | 311.01                             | 309.15                            | 1.86         |
| 85               | 300              | 733.5            | 11.01         | 372.83           | 265.23                             | 280.10                            | 14.87        |
| 85               | 364.7            | 817.6            | 7.77          | 422.43           | 285.33                             | 289.13                            | 3.8          |
| 105              | 105              | 679.4            | 30.0          | 296.47           | 331.63                             | 359.23                            | 27.6         |
| 105              | 144              | 723.5            | 26.77         | 324.17           | 334.95                             | 350.56                            | 15.61        |
| 105              | 205.9            | 791.2            | 22.17         | 367.37           | 340.42                             | 339.81                            | 0.61         |
| 105              | 264.7            | 817.6            | 17.67         | 395.77           | 325.81                             | 324.81                            | 1            |
| 105              | 323.5            | 832.3            | 12.98         | 420.27           | 307.00                             | 310.85                            | 3.85         |
| 105              | 347.1            | 852.9            | 11.51         | 435              | 308.30                             | 310.39                            | 2.09         |
| 125              | 125              | 723.5            | 30.0          | 324.5            | 345.54                             | 379.85                            | 34.31        |
| 125              | 164.7            | 785.3            | 26.93         | 358.33           | 358.67                             | 374.26                            | 15.59        |
| 125              | 182.4            | 826.5            | 25.78         | 377.97           | 372.61                             | 375.84                            | 3.23         |
| 125              | 255.9            | 867.6            | 20.5          | 416.17           | 357.19                             | 354.13                            | 3.06         |
| 125              | 352.9            | 905.9            | 13.52         | 461.27           | 332.56                             | 332.12                            | 0.44         |
| 125              | 420.6            | 932.4            | 8.789         | 492.67           | 319.18                             | 322.40                            | 3.22         |
| 145              | 145              | 800              | 30.0          | 363.33           | 378.16                             | 407.40                            | 29.24        |
| 145              | 250              | 900              | 22.63         | 431.67           | 377.72                             | 379.05                            | 1.33         |
| 145              | 300              | 935.3            | 19.34         | 460.1            | 372.21                             | 368.06                            | 4.15         |
| 145              | 400              | 982.4            | 12.72         | 509.13           | 352.00                             | 348.63                            | 3.37         |
| Average          |                  |                  |               |                  |                                    |                                   | 8.38         |

the test data. But temperature dependency, bedding plane orientation, shear plane orientation, and other anisotropic features of salt have been overlooked during development of the new failure criterion; more

efforts are required for better failure criterion based on more definite results.

- The Mohr–Coulomb criterion, which is one of the most trusted and widely used linear failure criteria for soils



**Table 4** The results of the true triaxial compressive tests for Mizuho trachyte conducted by Mogi (1979)

| Failure stresses |                  |                  | $\psi$<br>( $^{\circ}$ ) | $\sigma_m$ (MPa) | $\sqrt{J_2}$ (MPa)<br>Experimental | $\sqrt{J_2}$ (MPa)<br>Theoretical | Errors (MPa) |
|------------------|------------------|------------------|--------------------------|------------------|------------------------------------|-----------------------------------|--------------|
| $\sigma_3$ (MPa) | $\sigma_2$ (MPa) | $\sigma_1$ (MPa) |                          |                  |                                    |                                   |              |
| 45               | 45               | 297.39           | 30.00                    | 129.13           | 145.72                             | 144.13                            | 1.59         |
| 45               | 54.55            | 313.91           | 28.21                    | 137.82           | 149.79                             | 140.25                            | 9.54         |
| 45               | 70.92            | 326.09           | 25.22                    | 147.34           | 147.70                             | 134.85                            | 12.85        |
| 45               | 95.45            | 333.39           | 20.57                    | 157.95           | 138.91                             | 126.96                            | 11.95        |
| 45               | 141.8            | 348.7            | 11.82                    | 178.5            | 125.82                             | 117.57                            | 8.25         |
| 45               | 213.64           | 360.87           | -2.24                    | 206.50           | 109.39                             | 109.28                            | 0.11         |
| 45               | 289.09           | 365.22           | -16.8                    | 233.10           | 108.91                             | 107.71                            | 1.2          |
| 45               | 331.81           | 351.3            | -26.7                    | 242.70           | 117.63                             | 108.15                            | 9.48         |
| 60               | 60               | 339.13           | 30.00                    | 153.04           | 161.16                             | 160                               | 1.16         |
| 60               | 90.48            | 352.17           | 24.56                    | 167.55           | 151.60                             | 143.79                            | 7.81         |
| 60               | 141.9            | 382.61           | 15.87                    | 194.84           | 142.94                             | 132.39                            | 10.55        |
| 60               | 191.33           | 395.65           | 7.156                    | 215.66           | 129.58                             | 123.89                            | 5.69         |
| 60               | 228.37           | 404.35           | 0.73                     | 230.91           | 122.67                             | 120.24                            | 2.43         |
| 60               | 271.43           | 400              | -8.01                    | 243.81           | 113.84                             | 115.75                            | 1.91         |
| 60               | 331.43           | 382.61           | -21.5                    | 258.01           | 114.68                             | 113.01                            | 1.67         |
| 75               | 75               | 365.22           | 30.00                    | 171.74           | 167.56                             | 171.68                            | 4.12         |
| 75               | 114.29           | 400              | 23.64                    | 196.43           | 165.73                             | 155.31                            | 10.42        |
| 75               | 153.33           | 417.39           | 17.39                    | 215.24           | 155.77                             | 144.6                             | 11.17        |
| 75               | 228.57           | 438.26           | 5.10                     | 247.28           | 136.34                             | 131.36                            | 4.98         |
| 75               | 300              | 439.13           | -7.75                    | 271.38           | 122.02                             | 123.72                            | 1.7          |
| 75               | 342.86           | 424.35           | -17.1                    | 280.74           | 119.045                            | 120.42                            | 1.375        |
| 75               | 390.48           | 451.3            | -21.3                    | 305.59           | 133.50                             | 125.19                            | 8.31         |
| 100              | 137.4            | 460              | 24.58                    | 232.47           | 186.88                             | 176.1                             | 10.78        |
| 100              | 185.71           | 488.7            | 17.89                    | 258.14           | 178.40                             | 163.09                            | 15.31        |
| 100              | 274.29           | 493.91           | 3.80                     | 289.4            | 145.40                             | 142.41                            | 2.99         |
| 100              | 381.9            | 521.74           | -11.0                    | 334.55           | 140.58                             | 137.6                             | 2.98         |
| 100              | 411.43           | 513.04           | -16.3                    | 341.49           | 140.02                             | 135.86                            | 4.16         |
| Average          |                  |                  |                          |                  |                                    |                                   | 6.09         |

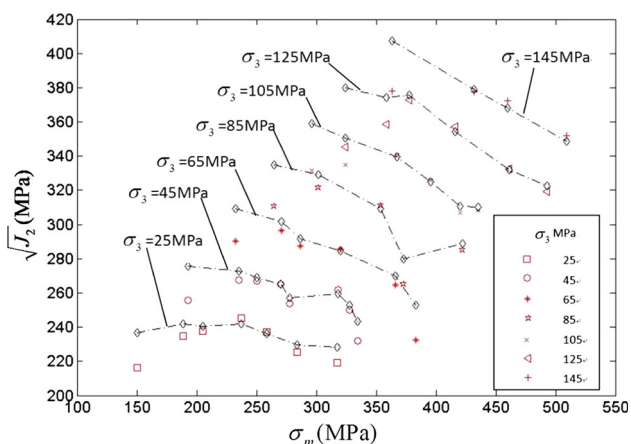


**Fig. 6** Comparisons between the true triaxial test data (points) of Dunham dolomite produced by Mogi and the non-linear triaxial shear energy yield criterion prediction (lines) in terms of  $\sqrt{J_2}$

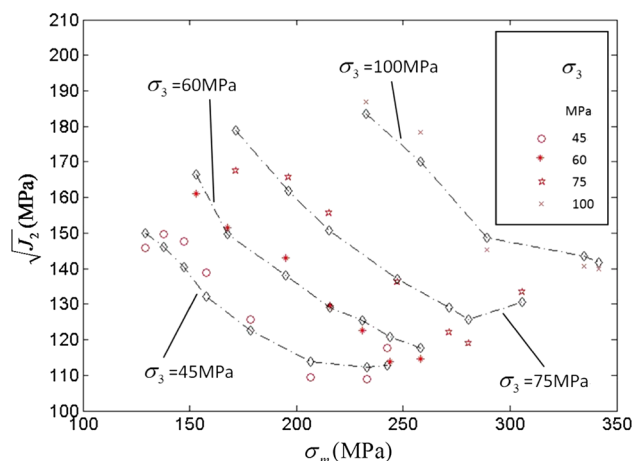


**Fig. 7** Comparisons between the true triaxial test data (points) of Mizuho trachyte produced by Mogi and the non-linear triaxial shear energy yield criterion prediction (lines) in terms of  $\sqrt{J_2}$

**Table 5** The results of the true triaxial compressive tests for Naxos marble conducted by Micheles (1985)

| Failure stresses |                  |                  | $\psi$<br>(°) | $\sigma_m$ (MPa) | $\sqrt{J_2}$ (MPa)<br>Experimental | $\sqrt{J_2}$ (MPa)<br>Theoretical | Errors (MPa) |
|------------------|------------------|------------------|---------------|------------------|------------------------------------|-----------------------------------|--------------|
| $\sigma_3$ (MPa) | $\sigma_2$ (MPa) | $\sigma_1$ (MPa) |               |                  |                                    |                                   |              |
| 0                | 3.45             | 60.7             | 27.10         | 21.38            | 33.08                              | 32.82                             | 0.26         |
| 0                | 10.34            | 76.9             | 22.88         | 29.08            | 38.66                              | 37.57                             | 1.09         |
| 0                | 20.34            | 105              | 19.48         | 41.78            | 49.58                              | 45.80                             | 3.78         |
| 0                | 34.47            | 103.3            | 10.87         | 45.92            | 42.16                              | 44.50                             | 2.34         |
| 3.45             | 3.45             | 66.3             | 30.00         | 24.4             | 36.29                              | 36.69                             | 0.4          |
| 3.45             | 5.17             | 75.1             | 28.80         | 27.91            | 40.38                              | 39.36                             | 1.02         |
| 3.45             | 6.89             | 83.9             | 27.83         | 31.41            | 44.48                              | 41.99                             | 2.49         |
| 3.45             | 10.34            | 94               | 26.08         | 35.93            | 48.38                              | 44.91                             | 3.47         |
| 3.45             | 27.58            | 129.8            | 19.64         | 53.61            | 59.83                              | 54.83                             | 5            |
| 3.45             | 68.95            | 192.7            | 10.08         | 88.37            | 76.29                              | 72.43                             | 3.86         |
| 3.45             | 82.74            | 143.3            | -4.42         | 76.50            | 47.65                              | 58.14                             | 10.49        |
| 6.89             | 6.89             | 83.8             | 30.00         | 32.53            | 44.40                              | 44.18                             | 0.22         |
| 6.89             | 13.79            | 112.8            | 26.66         | 44.49            | 57.23                              | 52.54                             | 4.69         |
| 6.89             | 27.58            | 134.1            | 21.28         | 56.19            | 62.08                              | 57.97                             | 4.11         |
| 6.89             | 55.16            | 191.6            | 15.41         | 84.55            | 81.20                              | 73.93                             | 7.27         |
| 6.89             | 82.74            | 188.1            | 5.371         | 92.58            | 68.26                              | 72.14                             | 3.88         |
| 6.89             | 110.31           | 174.6            | -7.67         | 97.27            | 56.22                              | 69.48                             | 13.26        |
| 13.79            | 13.79            | 115.9            | 30.00         | 47.83            | 58.95                              | 58.04                             | 0.91         |
| 13.79            | 20.68            | 126.3            | 26.87         | 53.59            | 61.04                              | 60.38                             | 0.66         |
| 13.79            | 27.58            | 147.2            | 24.61         | 62.86            | 69.29                              | 65.98                             | 3.31         |
| 13.79            | 41.37            | 154.8            | 19.37         | 69.99            | 66.45                              | 66.83                             | 0.38         |
| 13.79            | 55.16            | 196.4            | 17.52         | 88.45            | 83.28                              | 78.58                             | 4.7          |
| 13.79            | 82.74            | 254.4            | 13.85         | 116.98           | 103.03                             | 94.66                             | 8.37         |
| 13.79            | 110.31           | 278.1            | 8.85          | 134.07           | 104.58                             | 100.95                            | 3.63         |
| 20.68            | 20.68            | 138              | 30.00         | 59.79            | 67.73                              | 68.72                             | 0.99         |
| 20.68            | 27.58            | 150.2            | 27.29         | 66.15            | 70.85                              | 71.34                             | 0.49         |
| 20.68            | 62.05            | 208.7            | 17.92         | 97.14            | 86.34                              | 85.17                             | 1.17         |
| 20.68            | 82.73            | 260.2            | 15.55         | 121.20           | 105.55                             | 99.38                             | 6.17         |
| 20.68            | 110.31           | 289.1            | 10.86         | 140.03           | 109.52                             | 106.75                            | 2.77         |
| 27.58            | 27.58            | 170.6            | 30.00         | 75.25            | 82.57                              | 82.37                             | 0.2          |
| 27.58            | 48.26            | 166.6            | 22.08         | 80.81            | 68.84                              | 77.51                             | 8.67         |
| 27.58            | 55.16            | 222              | 22.47         | 101.58           | 96.98                              | 93.77                             | 3.21         |
| 27.58            | 82.73            | 274.8            | 17.73         | 128.37           | 113.15                             | 107.04                            | 6.11         |
| 27.58            | 110.31           | 314              | 13.70         | 150.63           | 122.35                             | 116.99                            | 5.36         |
| Average          |                  |                  |               |                  |                                    |                                   | 3.67         |

**Table 6** Fitting parameters of three types of rocks calibrated for the non-linear triaxial shear energy yield criterion

| Rock type       | Calibrated material parameters |       |       |        |       |       |       |
|-----------------|--------------------------------|-------|-------|--------|-------|-------|-------|
|                 | $\beta$                        | $N$   | $D_1$ | $D_2$  | $D_3$ | $D_4$ | $D_5$ |
| Dunham dolomite | 0.037                          | 0.64  | 0.555 | 25.744 | 1.665 | 6.661 | 0.961 |
| Mizuho trachyte | 0.022                          | 0.58  | 0.561 | 20.522 | 1.683 | 6.733 | 0.972 |
| Naxos marble    | 0.680                          | 0.951 | 0.337 | 31.141 | 1.009 | 4.038 | 0.583 |

and rocks, can be included in the triple shear energy yield criterion. The limit locus of the triple shear energy yield criterion in the deviatoric plane is circumscribed to the limit locus of the Mohr–Coulomb criterion. So the

Mohr–Coulomb criterion is more conservative than the triple shear energy yield criterion.  
 5. The parameters of the non-linear triple shear energy yield criterion can be determined from a conventional

triaxial compressive test. Therefore, it can be easily applied to analytical and numerical methods for rock mechanics and engineering associated with salt rock.

6. Comparative analysis for non-salt rocks confirms the availability of the non-linear triple shear energy yield criterion for non-salt rocks. In fact, the non-linear triple shear energy yield criterion reveals the rock's intrinsic response to shear fracture by energy method, so it can be seen as a general failure criterion for rocks which are fractured by shear stress.

**Acknowledgments** This study was financially supported by the National Nature Science Foundation of China (51225404), Shanxi Nature Science Foundation (2014011044-1), and San-Jin scholar support project, which are gratefully acknowledged.

## References

- Chang CD, Haimson B (2012) A failure criterion for rocks based on true triaxial testing. *Rock Mech Rock Eng* 45:1007–1010
- Coulomb CA (1776) Sur une application des regles maximis et minimis a quelques problems de statique, relatives a l'architecture. *Acad Sci Paris Mem Math Phys* 7:343–382
- DeVries KL, Mellegard KD, Callahan GD (2002) Salt damage criterion proof-of-concept research. Topical report RSI-1675/DE-FC26-00NT41026
- DeVries KL, Mellegard KD, Callahan GD, Goodman WM (2005) Cavern roof stability for natural gas storage in bedded salt. Topical report RSI-1829/DE-FG26-02NT41651
- Fuenkajorn K, Phueakphum D (2010) Effects of cyclic loading on mechanical properties of Maha Sarakham salt. *Eng Geol* 112:43–52
- Gao YF, Tao ZY (1993) Examination and analysis of true triaxial compression testing of strength criteria of rock. *Chin J Geotech Eng* 15(4):26–32
- Gao H, Zheng YR, Feng XT (2007) Study on energy yield criterion of geomaterials. *Chin J Rock Mech Eng* 26(12):2437–2443
- Haimson BC, Chang C (2000) A new true triaxial cell for testing mechanical properties of rock, and its use to determine rock strength and deformability of Westerly granite. *Int J Rock Mech Min Sci* 37:285–296
- Handin J, Heard HC, Magouirk JN (1967) Effect of the intermediate principal stress on the failure of limestone, dolomite and glass at different temperatures and strain rates. *J Geophys Res* 72:611–640
- Hatzor YH, Heyman EP (1997) Dilation of anisotropic rock salt: evidence from mount sedom diapir. *J Geophys Res* 102(B7):14853–14868
- Hunsche U (1993) Failure behaviour of rock around underground cavities. In: Proceedings of 7th symposium on salt, Kyoto International Conference Hall, vol 1, April 6–9, Kyoto. Elsevier Science Publishers B.V., Amsterdam, pp 59–65
- Hunsche U, Albrecht H (1990) Results of true triaxial strength tests on rock salt. *Eng Fract Mech* 35(4/5):867–877
- Lade P, Duncan J (1975) Elasto-plastic stress–strain theory for cohesion less soil. *J Geotech Eng Div ASCE* 101:1037–1053
- Lee H, Haimson B (2011) True triaxial strength, deformability, and brittle failure of granodiorite from the San Andreas Fault Observatory at Depth. *Int J Rock Mech Min Sci* 48:1199–1207
- Liang WG, Yang CH, Zhao YS, Dusseaultc MB, Liu J (2007) Experimental investigation of mechanical properties of bedded salt rock. *Int J Rock Mech Min Sci* 44:400–411
- Liang WG, Zhao YS, Xu SG, Dusseaultc MB (2011) Effect of strain rate on the mechanical properties of salt rock. *Int J Rock Mech Min Sci* 48:161–167
- Liu XY, Ma LJ, Ma SN, Zhang XW, Gao L (2011) Comparative study of four failure criteria for intact bedded rock salt. *Int J Rock Mech Min Sci* 48:341–346
- Ma LJ, Liu XY, Wang MY et al (2013) Experimental investigation of the mechanical properties of rock salt under triaxial cyclic loading. *Int J Rock Mech Min Sci* 62:34–41
- Michelis P (1985) Polyaxial yielding of granular rock. *J Eng Mech* 111(8):1049–1066
- Mogi K (1979) Flow and fracture of rocks under general triaxial compression. In: Proceedings of the fourth international congress on rock mechanics, vol 3. AA Balkema, Montreal, pp 123–30
- Oku H, Haimson B, Song S-R (2007) True triaxial strength and deformability of the siltstone overlying the Chelungpu fault (Chi–Chi earthquake), Taiwan. *Geophys Res Lett* 34:L09306
- Ratigan JL, Vogt TJ (1991) A note on the use of precision level surveys to determine subsidence rates. *Int J Rock Mech Min Sci* 28(4):337–341
- Spiers CJ, Peach CJ, Brzesowsky RH et al (1988) Long term rheological and transport properties of dry and wet salt rocks. EUR 11848, University of Utrecht, Utrecht
- Sriapai T, Walsri C, Fuenkajorn K (2013) True-triaxial compressive strength of Maha Sarakham salt. *Int J Rock Mech Min Sci* 61:256–265
- Yu MH, Zan YW, Zhao J, Yoshimine M (2002) A unified strength criterion for rock material. *Int J Rock Mech Min Sci* 39:975–989
- Zheng YR, Kong L (2010) Geotechnical plastic mechanics. Architecture and Building Press, Beijing, pp 79–88 (in Chinese)